Dislocations Deflect and Perturb Dynamically Propagating Cracks

Dov Sherman and Ilan Be'ery

Department of Materials Engineering, Technion-Israel Institute of Technology, Haifa 32000, Israel

(Received 23 March 2004; published 21 December 2004)

We demonstrate that in single-crystal silicon short-range collisions of a dynamically propagating crack with stationary, intrinsic, ''inclined'' dislocations generate local crack deflections that grow to a large surface perturbation. Experiments show that when the crack collides with a single dislocation, the perturbation height is about 8 nm, but when it collides with a group of adjacent dislocations, the perturbation may extend to 80 nm in height ($\sim 200|\vec{b}|$) and 250 μm in length, visible to the naked eye. A model was developed formulating the maximum velocity at which the crack climbs into the dislocation's core. The model predicts that when a dislocation's line is perpendicular to the crack surface, no interaction takes place.

DOI: 10.1103/PhysRevLett.93.265501 PACS numbers: 62.20.Mk, 68.35.Gy, 81.40.Np

Dynamically propagating cracks in brittle crystals are atomistically smooth, provided the crack velocity is within $0.4C_R$ (C_R being the Rayleigh free surface wave speed). Causes of perturbations along the fracture surface in brittle crystals have recently been investigated experimentally [1–3], numerically [4–8], and theoretically [9–11]. It was found that surface perturbations are triggered by dynamic instabilities at higher velocities or by asperities, or result from wave propagation. Several aspects of intrinsic defects in brittle crystals, such as dislocations, as the source for surface perturbations have been investigated. For example, the coupling between a screw dislocation's shear stress and the crack's tensile stress is responsible for the ''softening effect'' during interaction [12]; the dislocation's high shear stress may reduce the cohesive energy of the cleavage plane of the deflected crack, and the high tensile stresses generated by the crack may reduce the resolved shear stresses of the slip plane. The ''shielding effect'' of a sufficiently closed dislocation near the crack tip was identified [13]; the dislocation may shield or antishield the toughness of the material. One crack deflection mechanism was discussed almost four decades ago [14]; it was suggested that a screw dislocation located perpendicularly to a crack plane generates a single Burger's vector step on the crack plane at the point of intersection. Large perturbations can be produced only if many steps of the same sign combine; but such an occurrence has never been detected experimentally. Recently, however, detectable surface perturbations have been demonstrated; they where generated in a silicon crystal during the interaction of a running crack with a stationary dislocation located parallel to the direction of the crack's propagation [15]. When the distance of the dislocation line from the crack surface is smaller than a certain critical length, the crack deflects into the dislocation's core, and the energy released from the relaxed dislocation's core is consumed by the new free surfaces of the deflected crack. In the current contribution we describe and analyze a more complex and general case of interaction, in which a fast moving crack collides with a screw dislocation inclined to the crack surface; resulting in the crack's deflection and the generation of large surface perturbations.

We have recently shown that in thin, strip-shaped specimens (cut from [001] wafers) subjected to three-point bending (3PB), the cleavage plane of propagation in defect-free silicon crystals is dictated by the crack velocity [16,17]. Slower cracks propagate along the perpendicular, {110} cleavage plane, faster cracks along the inclined, {111} plane [Fig. 1(a)]. The fast cracks along the {111} plane generate large surface perturbations [18–20], which prevent visualization of the perturbations generated when the crack collides with dislocations. It was therefore decided to examine a collision on the ''slow'' {110} plane which, in defect-free silicon, exhibits an atomistically smooth fracture surface [21]. The shape of the crack front as it propagates in the specimen is that of a quarter ellipse [Fig. 1(b)] [22]. The parallel velocity at the bottom surface of the specimens, V_x, was measured using the potential drop technique [23]. It is emphasized that the velocity normal to the crack front, V_n, is the important one in these specimens, since it is the actual bond-breaking velocity. That velocity is highest at the bottom of the specimen's surface (of the order of 1500 m/sec in our specimens) Fig. 1(b), but decreases to about 30 m/sec close to the top surface [16,17].

Thin wide strip-shaped specimens were cut from [001] defect-free silicon wafers, 100 mm in diameter and 525 μm thick. In order to study the collisions of a dynamic crack with stationary inclined dislocations, these were created by plastic deformations in the form of slip bands of dislocations induced in the specimens prior to 3PB. This was achieved by subjecting the specimens to uniaxial pressure of up to 10 MPa in the [001] direction at a temperature of 900 °C for up to 10 min. The specimens were then notched to a length of 0.5 to 1 mm with a 150 μm thick diamond saw and fractured under 3PB loading [Fig. 1(a)]. One half of each specimen was used to expose the site of the dislocations by etch pits [24], the other was subjected to high-resolution electron microscopy

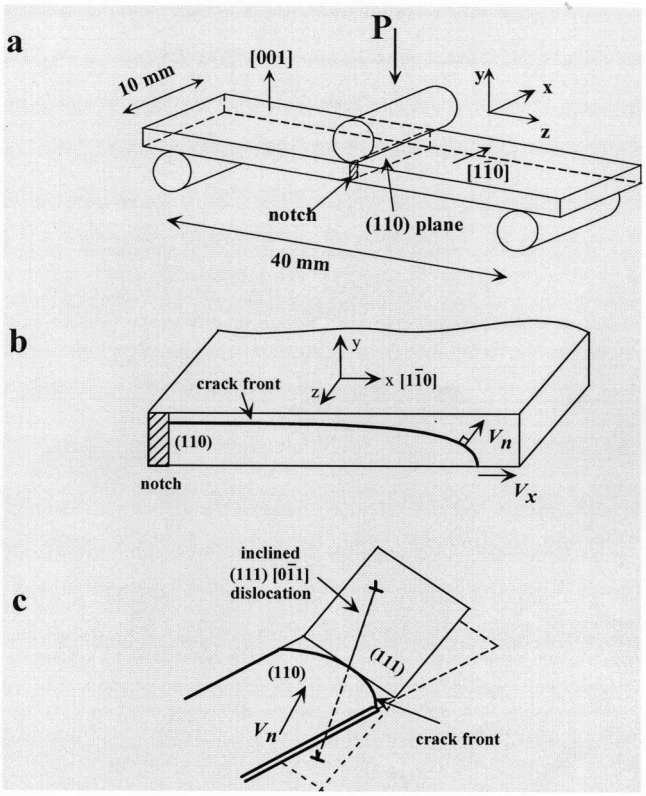

FIG. 1. (a) Three-point-bending (3PB) loading of a thin wide specimen, notched at one edge, (b) the shape of the crack front [20], and (c) the schematics of the inclined dislocation line [belonging to the (111) plane] with respect to the crack surface.

(HRSEM) and atomic force microscopy (AFM) analyses of the fracture surface. Specimens of a ''control'' group cut from the same wafers, but with no dislocations induced, were fractured along the (110) cleavage plane and analyzed using HRSEM and AFM. They exhibited atomistically smooth surfaces.

Since the energy of screw dislocations is about half that of edge dislocations, the former are the ones occurring preferably in silicon [25,26], and the dislocations in our analysis are therefore of the screw type, belonging to the $\{111\}\langle 110\rangle$ family; 12 lines—three $\langle 110\rangle$ dislocation lines in each of the four $\{111\}$ planes. However, only two of these dislocation lines on each plane can collide with a fast moving crack on the (110) surface, e.g., $(111)\times[0\bar{1}1]$ [see Fig. 1(c)] and $(111)[0\bar{1}\,\bar{1}]$. In the former, the crack deflects ''upwards,'' in the latter—''downwards.'' The third dislocation line is either parallel or perpendicular to the (110) plane and is therefore not considered as ''inclined.''

Special care was taken to assure that crack deflection and surface perturbations were initiated by collisions with dislocation, and we demonstrate this conclusively in the following. An optical microscope micrograph of a slightly etched fracture surface proves that each perturbation originated at a dislocation site, as shown by arrows in Fig. 2(a). An optical micrograph with higher magnification of the second half of the fractured specimen reveals the surface perturbations along the (110) surface in that specimen (see arrows in Fig. 2(b)]. Note the smeared surface in the zone of high dislocation line density. Isolated dislocation were designated A. An AFM micrograph of a single, small perturbation is shown in Fig. 2(c), that of a large perturbation—in Fig. 2(d). The height of the latter is approximately 80 nm, which is about $200|\bar{b}|$. Note that the perturbation generated during collision with a single dislocation has a similar shape but is of a smaller size, its height being nearly 8 nm. A possible explanation for the large height of the perturbations lies in the coupling between the screw dislocation's shear stress and the crack's tensile stress, known as the ''softening effect'' (see above) [12].

The $(111)[0\bar{1}1]$ dislocation line that interacts with the propagating crack [Fig. 1(c)] is inclined at an angle, $\delta = 60°$ to the (110) plane, as shown in Fig. 3(a), while the projection of that line on the (110) plane and to the $[1\bar{1}0]$ direction is at an angle, $\beta = 54.7°$. The normal velocity, V_n, [Figs. 1(b), 2(b), and 3(a)] obeys $V_n = V_x\cos\theta$. Assuming continuity of the crack front during climbing, the normalized climbing velocity can be defined as

$$\frac{V_{CL}}{V_x} = \frac{\cos\theta}{\cos(\beta-\theta)\cos\delta}, \tag{1}$$

where θ is the angle of the normal-velocity vector along the quarter-elliptical crack front with respect to the $[1\bar{1}0]$ direction [22]. Figures 2(b) and 3(a), and obeying $\theta = tg^{-1}[(0.8h/3h)^2(x/y)]$, where h is the thickness of the specimen and x and y are the coordinates along the crack

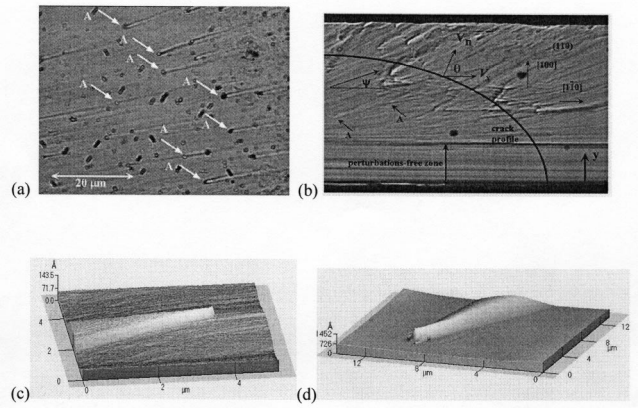

FIG. 2. (a) Optical microscope micrograph of a slightly etched (110) fracture surface, (b) Optical photograph of the (110) surface, with the quarter-elliptical crack front (note the large perturbations-free zone), (c) AFM micrograph of a small perturbation resulting from interaction with a single perturbation (velocity vector from right to left), and (d) large perturbation resulting from interaction with several adjacent dislocations (velocity vector from left to right).

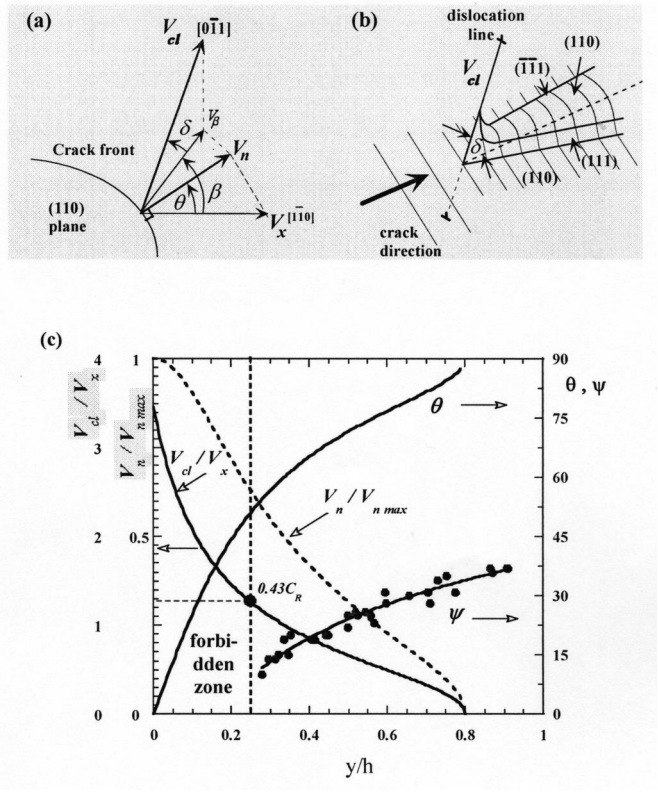

FIG. 3. (a) The velocity, V_{CL}, at which the climbing crack penetrates into the dislocation core and the associated angles and velocities. (b) Schematic view of the perturbation. (c) The intersection of the normalized climbing velocity, V_{CL}, Eq. (1), and the ''forbidden zone,'' the angle of propagation of an individual perturbation (ψ) compared with the local velocity vector's direction (θ) at interaction, and the normalized normal velocity at the normalized coordinate y/h.

front. The normalized velocity, Eq. (1), is plotted in Fig. 3(c) as a function of the normalized position, y/h.

Observation of the (110) fracture surface reveals a zone that is free of large surface perturbations resulting from collisions with inclined dislocations. This zone is at the bottom of the fracture surface, shown in Fig. 2(b), where V_n is high. We term this zone as a (large) perturbations-free zone. The measured length of this zone is $y = 0.25h$, and is shown by the dashed line in Fig. 3(c). The maximum velocity at which the crack is climbing into the dislocation's core is defined at the point of intersection, Fig. 3(c). For $V_x = 1500$ m/sec, the maximum climbing velocity is $V_{CL}^{\max} = 1950$ m/sec. The Rayleigh surface wave speed at 60° along the (111) plane is $C_R = 4530$ m/sec [27], which yields

$$V_{CL}^{\max} = 0.43 C_R. \tag{2}$$

To the best of our knowledge, this is the first time the maximum climbing velocity has been evaluated. The physical meaning of this is that in this zone the crack cuts through the dislocations. As the parallel velocity, V_x, drops, the perturbations-free zone is expected to be reduced in length. An important consequence of this analysis is the verification of the velocity, V_{CL}, of a crack climbing into perpendicular dislocations [for example, the $(1\bar{1}1) \times [110]$ dislocation]. In this case the angle of dislocation with the $[1\bar{1}0]$ direction, β, coincides with θ, Fig. 3(a), and the angle of the dislocation with the (110) surface is $\delta = 90°$. Substituting these values into Eq. (1) yields an infinite climbing velocity regardless of θ. We therefore postulate that the collision of a dynamically propagating crack with perpendicular dislocations causes no large surface perturbation to the extent described in this work (a Burger's vector step as was described in Ref. [14], and mentioned above, is likely), and the crack cuts through the dislocation line. This result can be verified by considering the elastic fields of a perpendicular dislocation, which are symmetrical with respect to the crack surface. The interaction of the crack with such a dislocation leads to only a limited energy that is released from the dislocation's core, presumably responsible for a Burger's vector-size step; a large deflection, as described in this work, is physically avoided. We further suggest that the ''softening effect'' [12] for perpendicular dislocation lines is avoided due to the perpendicularity between the tensile stresses at the crack tip and the shear stresses at the dislocation's core.

The AFM, with its 50 nm tip radius, fails to describe the exact shape of the perturbations at their edges. We accordingly suggest the shape shown in Fig. 3(b). Generation of the cometlike perturbations is described herein: When the crack collides with the inclined dislocation's core, it cuts the core's atomic bonds, and the atomic disorder vanishes. The strain energy in the core is released in that portion of the dislocation, to be consumed in the generation of the new free surfaces, the ''side walls'' of the perturbation. After reaching the maximum height, the crack is detached from the dislocation line. Thereafter there is a gradual reduction in the perturbation's height. The ''side walls,'' having a cross section of nearly trapezoidal shape with a slightly curved upper surface, propagate by atomistic steps on the (111) and the $(\bar{1}\,\bar{1}\,1)$ planes, as shown in Fig. 3(b). This was detected by AFM [Figs. 2(c) and 2(d)]. It is an important observation that the perturbations are nearly straight, propagating at an angle ψ with respect to the $[1\bar{1}0]$ direction, and are presumably smooth, which suggests that the crack path in single-crystal silicon may be constructed from atomistically smooth steps. Atomistically smooth and curved crack paths have recently been described elsewhere [28].

We further suggest that the angle of propagation of a perturbation, ψ, is determined by equilibrium between two opposing mechanisms, namely, the direction of the local normal velocity and the natural tendency of the perturbation to propagate on the (111) and $(\bar{1}\,\bar{1}\,1)$ planes. We measured the value of this angle with respect to the $[1\bar{1}0]$

direction and its normalized initiation point, y/h. The variations of ψ and θ with the normalized position are shown in Fig. 3(c). The normalized normal velocity $(V_n/V_{n\max})$ is also shown in Fig. 3(c). The latter demonstrates the influence of the velocity vector, direction, and magnitude, on the angle of propagation of the perturbations. Note the relationship between these two angles, which is nearly 1:2.

The great extent of the perturbations is explained by the slow reduction of the perturbation's surfaces during crack propagation. Its finite extent is determined by the reduction of the kinetic energy and the fracture energy as the (normal) velocity decreases. In the lower portion of the cross section, where the normal velocity is high, the perturbations decay after reaching a length of about 250 μm. Much shorter perturbations, only 40 μm in length, were observed in the higher portion of the cross section, where the normal crack velocity is nearly a few tens of m/sec.

In summary, we have shown the fundamental phenomenon of crack deflection in single-crystal silicon when a dynamically propagating crack collides with stationary, intrinsic, and inclined screw dislocations, leading to high and long surface perturbations due to that collision, although the crack detached the dislocation line at the beginning of collision. The crack climbs into the dislocation core and relaxes its strain energy which, in turn, is consumed by creating new free surfaces of the crack. The maximum climbing velocity is about $0.43C_R$. At higher velocities, the crack will cut through the dislocation line, resulting in a large perturbations-free zone. It was also shown that dislocation lines perpendicular to the crack's plane cause no large surface perturbations.

Surface perturbations generated during the propagation of a dynamic crack are an important phenomenon in brittle single crystals. A fundamental aspect, which is far from being understood, is the dynamic of crack front propagation under repeated interaction with material imperfections such as dislocations. The results presented here can serve to gain a better understanding of the general phenomena related to crack deflections and surface perturbations during the propagation of a dynamic crack. They can also aid in theoretical calculations and in numerical analysis, such as molecular dynamics, in particular.

[1] J. Fineberg, S. P. Gross, M. Marder, and H. L. Swinney, Phys. Rev. Lett. **67**, 457 (1991).

[2] J. A. Hauch, D. Holland, M. P. Marder, and H. L. Swinney, Phys. Rev. Lett. **82**, 3823 (1999).

[3] T. Cramer, A. Wanner, and P. Gumbsch, Phys. Rev. Lett. **85**, 788 (2000).

[4] F. F. Abraham, D. Brodbeck, R. A. Rafey, and W. E. Rudge, Phys. Rev. Lett. **73**, 272 (1994).

[5] F. F. Abraham, N. Bernstein, J. Q. Broughton, and D. Hess, MRS Bull. **25**, 27 (2000).

[6] M. Marder, and S. Gross, J. Mech. Phys. Solids **43**, 1 (1995).

[7] P. Gumbsch, S. J. Zhou, and B. L. Holin, Phys. Rev. B **55**, 3445 (1997).

[8] D. Holland, and M. Marder, Phys. Rev. Lett. **80**, 746 (1998).

[9] S. Ramanathan and D. S. Fisher, Phys. Rev. Lett. **79**, 877 (1997).

[10] S. Ramanathan, and D. S. Fisher, Phys. Rev. B **58**, 6026 (1998).

[11] J. R. Willis, and A. B. Movchan, J. Mech. Phys. Solids **45**, 591 (1997).

[12] K. S. Cheung, A. S. Argon, and S. Yip, J. Appl. Phys. **69**, 2088 (2001); J. R. Rice, J. Mech. Phys. Solids **40**, 239 (1992); J. R. Rice, G. E. Beltz, and Y. Sun, in *Topics in Fracture and Fatigue*, edited by A. S. Argon (Springer Verlag, New York, 1992); Y. M. Sun, G. E. Beltz, and J. R. Rice, Mater. Sci. Eng. A **170**, 67 (1993).

[13] J. Weertman, *Dislocation Based Fracture Mechanics* (World Scientific Publishing, Singapore, 1998); J. R. Rice and R. M. Thomson, Philos. Mag. **29**, 73 (1974); M. A. Loyola de Oliveira and G. Michot, Mater. Sci. Eng. A **176**, 139 (1994).

[14] J. Friedel, *Dislocations* (Addison-Wesley Publishing Company, London, 1967).

[15] D. Shilo, D. Sherman, I. Be'ery, and E. Zolotoyabko, Phys. Rev. Lett. **89**, 235504 (2002).

[16] D. Sherman, and I. Be'ery, Scr. Mater. **49**, 551 (2003).

[17] D. Sherman, and I. Be'ery, J. Mech. Phys. Solids **52**, 1743 (2004).

[18] D. Sherman, and I. Be'ery, Phys. Rev. Lett. **80**, 540 (1988).

[19] D. Sherman, and I. Be'ery, Physica (Amsterdam) **119D**, 424 (1998).

[20] D. Sherman, and I. Be'ery, Physica (Amsterdam) **190D**, 177 (2004).

[21] I. Be'ery, U. Lev, and D. Sherman, J. Appl. Phys. **93**, 2429 (2003).

[22] D. Sherman, and I. Be'ery, J. Mater. Res. **18**, 2379 (2003).

[23] B. Stalder, P. Beguelin, and H. H. Kausch, Int. J. Fract. **22**, R47 (1983).

[24] F. Secco d'Aragona, Phys. Status Solidi A **7**, 577 (1971).

[25] W. Cai, V. V. Bulatov, J. Chang, J. Li, and S. Yip, Phys. Rev. Lett. **86**, 5727 (2001).

[26] A. S. Nandedkar and J. Narayan, Philos. Mag. A **56**, 625 (1987).

[27] H. Coufal, K. Meyer, R. K. Grygier, P. Hess, and A. Neubrand, J. Acoust. Soc. Am. **95**, 1158 (1994).

[28] R. D. Deegan, S. Chheda, L. Patel, M. Marder, H. L. Swinney, J. Kim, and A. deLozanne, Phys. Rev. E **67**, 066209 (2003).